Agri. & Biosys. Eng. Vol. 1(1):22-29(2000)

Optimization of Finite Element Retina by GA for Plant Growth Neuro Modeling

H. Murase

Abstract: The development of bio-response feedback control system known as the speaking plant approach has been a challenging task for plant production engineers and scientists. In order to achieve the aim of developing such a bio-response feedback control system, the primary concern should be to develop a practical non-invasive technique for monitoring plant growth. Those who are skilled in raising plants can sense whether their plants are under adequate water conditions or not, for example, by merely observing minor color and tone changes before the plants wilt. Consequently, using machine vision, it may be possible to recognize changes in indices that describe plant conditions based on the appearance of growing plants. The interpretation of image information of plants may be based on image features extracted from the original pictorial image.
In this study, the performance of a finite element retina was optimized by a genetic algorithm. The optimized finite element retina was evaluated based on the performance of neural plant growth monitor that requires input data given by the finite element retina.
Keywords: Computer Vision, Finite Element Method, Neural Networks, Genetic Algorithm

Introduction

In a protected plant production system such as a plant factory, the control applications are limited to the programmed fixed command controls for environmental factors. The feedback control technology for greenhouse environmental factors such as temperature, humidity, radiation intensity, carbon dioxide concentration and so forth has been developed and successfully implemented (Hashimoto and Nonami, 1992). The development of bio-response feedback control system has been a challenging task for plant production engineers and scientists. Plant growth can be optimized or controlled by adjusting the environmental factors. Fig. 1 shows the neural network adaptive control system with a bio-response feedback loop containing another neural network which converts the pictorial information of plants into plant growth indices for evaluating the plant growth status. The control element of this system is the environment surrounding the plant consisting of temperature, humidity, CO_2 concentration, light intensity, and water potential of the root zone.

The practice of non-invasive measurements for plants is essential for the bio-information feedback and/or feed-forward control system of a plant factory. Those who are skilled in raising plants can sense whether their plants are under adequate water conditions or not, for example, by merely observing color and tone changes before the plants wilt. Hence, using machnie vision, it may be possible to recognize changes in indices that describe plant conditions based on the appearance of growing plants by machine vision. The interpretation of image information of plants may be based on image features extracted from the original pictorial image. Changes in plant size due to the growth reflect tonal variations over the plant canopy. The tonal variation can be transformed into pictorial information electronically in retrieval form. The textural analysis can be considered as one of applicable techniques for extracting image features (Murase et al., 1994; Haralick et al. 1973). Some of problems in implementing the textural analysis are that there is too much flexibility to construct the co-occurrence matrix and that the construction of the co-occurrence matrix requires impractical long calculation time. Broadly speaking, image features are any extractable measurement of use. Examples of low-level image features are pixel intensities or geometric distances between pixels. Features may also result from applying a feature extraction algorithm or operator to the image data.

Murase et al. (1996) introduced the finite element retina and made comparisons of performance of image features extraction between the finite element and the textural features. Murase and Nishiura (1996) reported that the performance of the finite element retina can be improved by arranging the location of choroidal cells and the optic nerve cells and the distribution of information conductivities in such a way that the potential gradient over the retinal plane is steep.

In this study, the performance of the finite element retina was optimized by a genetic algorithm. The optimized finite element retina was evaluated based on the performance of a neural plant growth monitor that

The author is **Haruhiko Murase**, Professor, Graduate School of Agriculture and Biological Sciences, Osaka Prefecture University, Japan. **Corresponding author**: Haruhiko Murase, Professor, Graduate School of Agriculture and Biological Sciences, Osaka Prefecture University 1-1, Gakuen, Sakai 593 Japan; e-mail:hmurase@bics.envi.osakafu-u.ac.jp

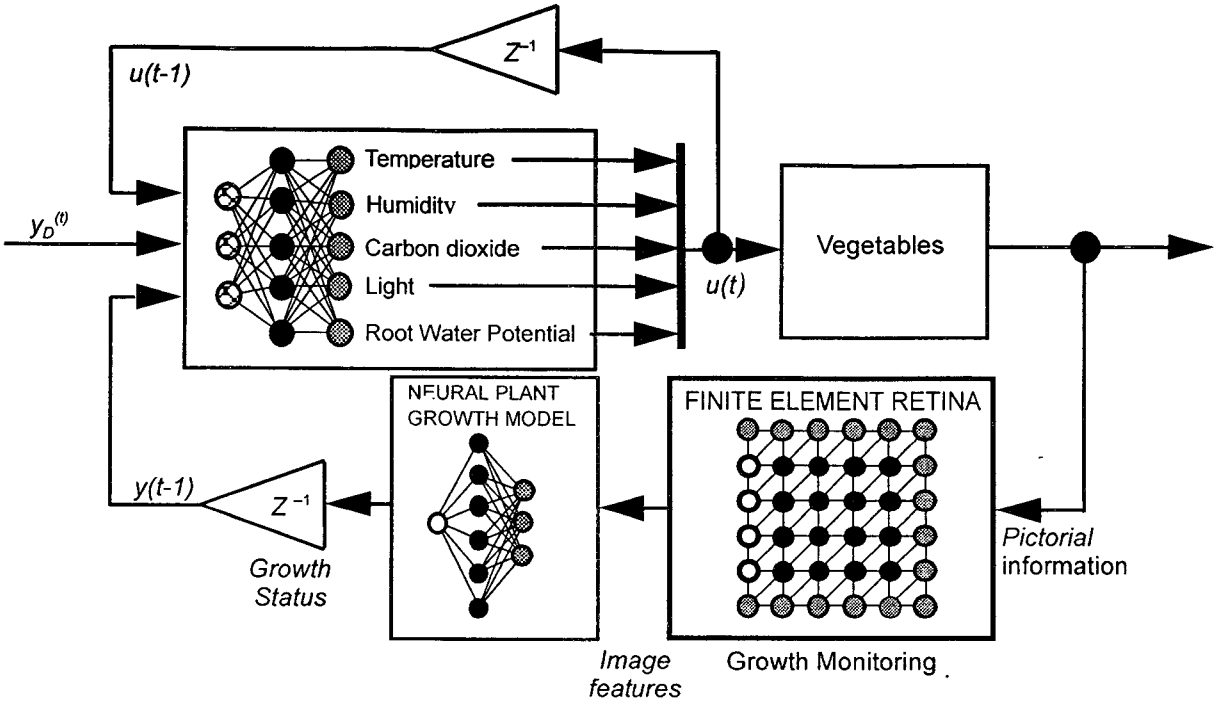

Fig. 1 Finite element retina and neural network models in the bio-response feedback loop.

requires input data given by the finite element retina. This is because a better finite element retina provides better data in terms of resolution for the neural plant growth monitor.

Materials and Methods

1. Finite Element Retina

The machine vision system for monitoring of plants growth (fig. 2) consist of the scene, vision hardware, calibration processor, image feature extraction processor, growth index evaluation processor and the control system. The image of a plant canopy or a community of plants is captured by the vision system. The raw data of the calibrated image is fed into the finite element retina. The output from the finite element retina is then directed to the neural plant growth model. Because of the large number of parameter involved in evaluating the plant growth, a neural network is used. The current growth indices of plants are compared with the reference input (set value) of growth indices. Then, deviation from normal appearance is calculated.

The basic mechanism of Finite Element Retina proposed by Murase et al. (1995) for generating image features is the conversion of incident light intensity distribution projected over the area comprising of finite element input nodes into a vector form of image features distributed over the output nodes. Fig. 3 is a conceptual representation of the finite element retina. The pictorial image of the object is projected over a finite element grid (meshed area) which is considered as retina. The boundary of the finite element grid

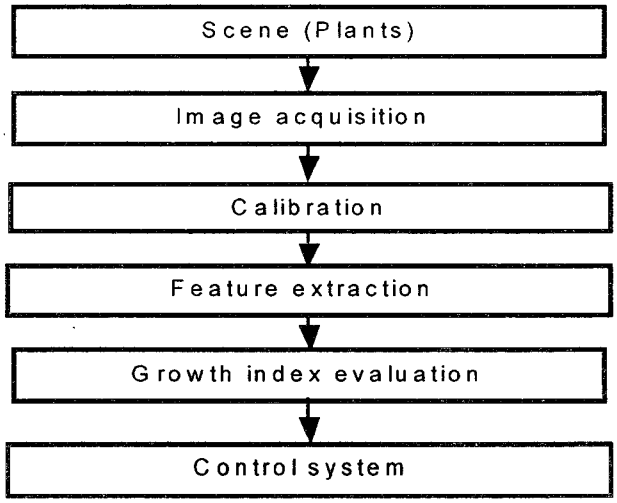

Fig. 2 Process of machine vision monitoring of plant growth.

where the outputs are retrieved serves as the optic nerve of a human eye. The other part of the boundary is a choroid.

Fig. 4 shows a schematic representation of the finite element retina that converts pictorial image into non-geometric image features numerically. This non geometric image feature can be calculated based on the differences of gray level between every input node of the finite element grid. Each input node serves as a photosensitive receptor (retinal cells). In practice, for instance, signals transferred from sensing elements of CCD area array should be given to these input nodes.

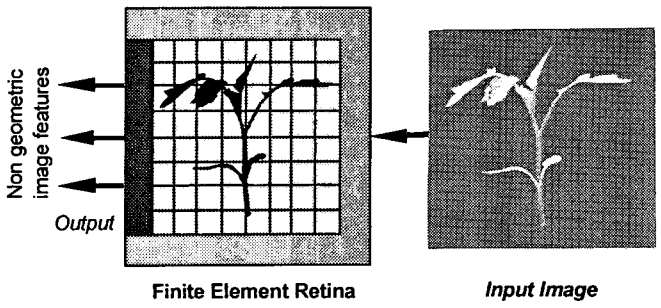

Fig. 3 Apparent function of finite element retina.

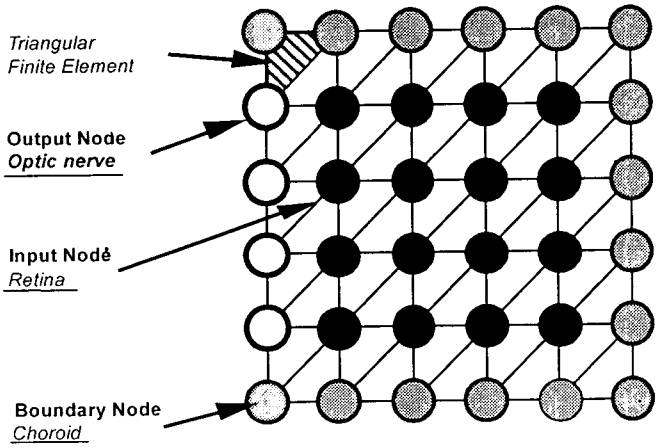

Fig. 4 Schematic representation of the finite element retina.

Nodal values of the output nodes (Optic nerve cells) become the finite element features. Other nodes are boundary nodes (Choroidal cells) on which boundary conditions are specified.

The algorithm to relate input and output signals of the finite element retina can be a linear mapping as described by a linear finite element equation. In this research work, a 2-D Poisson's equation was utilized as a governing equation given by eq.(1). The finite element equation used here is expressed as eq.(2). The basic mechanism of the finite element image processing grid for generating image features is the conversion of incident light intensity distribution projected over the area comprising of finite element input nodes into a vector form of image features distributed over the output nodes.

$$kx\frac{\partial^2}{\partial^2_x} + Ky\frac{\partial \phi^2}{\partial^2_y} = Q \qquad (1)$$

K_x : information conductivity in x direction
K_y : information conductivity in y direction
ϕ : potential
Q : onstant

$$[K]^{-1}\begin{bmatrix}\vdots\\A\\\vdots\\B\\C\\\vdots\end{bmatrix} = \begin{bmatrix}1\\\vdots\\2\\\vdots\\3\end{bmatrix} \qquad (2)$$

$[K]^{-1}$: inverse matrix of stiffness matrix
{A} : input vector
{1} : output vector (image features)

2. Optimization of Finite Element Retina

The performance or specification of the finite element retina can be set by determining K values and the node arrangements. The choice of K values and the node arrangements determines the sensitivity of the retina. The K value is usually uniform and taken as unity. The number of nodes depends on allowable calculation capacity. The arrangement of nodes is arbitrary. However, some trial procedure has been required to optimize the retinal performance .

Structure of Finite Element Retina

Fig. 5 illustrates the structure of a finite element retina which was subjected to the optimization. The sensing receptor is a five by five finite element nodal array. The sensing receptor consists of 25 input nodes. The receptor is surrounded by 24 boundary cells or nodes. Some of the boundary cells are designated as choroidal cells in the optimization process. The remaining cells can be used as work cells or output nodes. In this study, the K value was taken as unity.

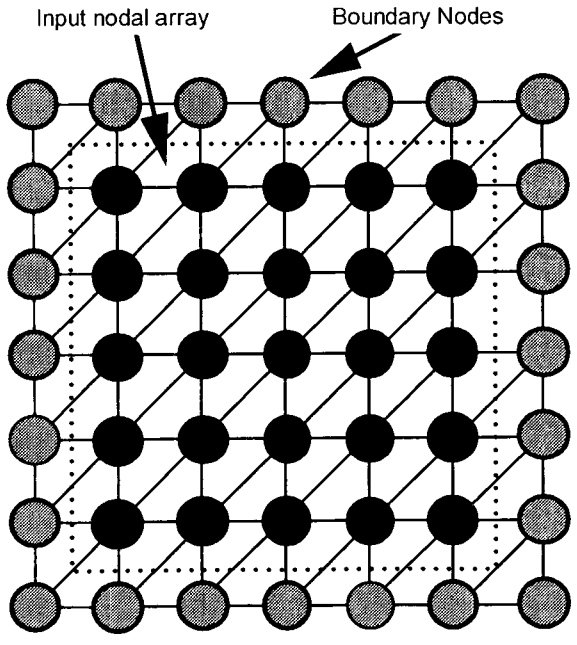

Fig. 5 The finite element retina used for optimization.

Optimization by a Genetic Algorithm

In this study, the Simple Genetic Algorithm (SGA) was used. The SGA starts by randomly generating a population of N individuals (chromosomes), that is, individual solutions. These individuals are evaluated for their fitness. Individuals with higher fitness scores are selected, with replacement, to create a mating pool of size N. This method of selection is called fitness proportionate reproduction. The genetic operators of crossover and mutation are applied at this stage in a probabilistic manner which results in some individuals from the mating pool to reproduce. The assumption here is that each pair of parents produces only one pair of offspring through the crossover operation. Now the population pool contains some individuals who never got a chance to reproduce and the offspring of those who got a chance to reproduce. The procedure continues until a suitable termination condition is satisfied. In this study, N was set at 50.

The performance of the finite element retina was optimized based on its sensitivity. The sensitivity can be evaluated by the ratio of the change in output level of the finite element retina to the change in input level of the retina. The fitness of a chromosome is evaluated for higher sensitivity. The number of work cells (output nodes) was limited to 3 out of 24 boundary cells in this study. The number of choroidal cells (up to 21 cells) and their locations together with the locations of 3 work cells were subjected to the optimization. The remaining boundary cells were left as general nerve cells. Fig. 6 illustrates the chromosome consisting of 3 five bits genes for work cell locations and 6 four bits genes for choroidal cell locations and one additional gene for the fitness level. The crossover operates only on the four bits genes except genes where the work cells are located.

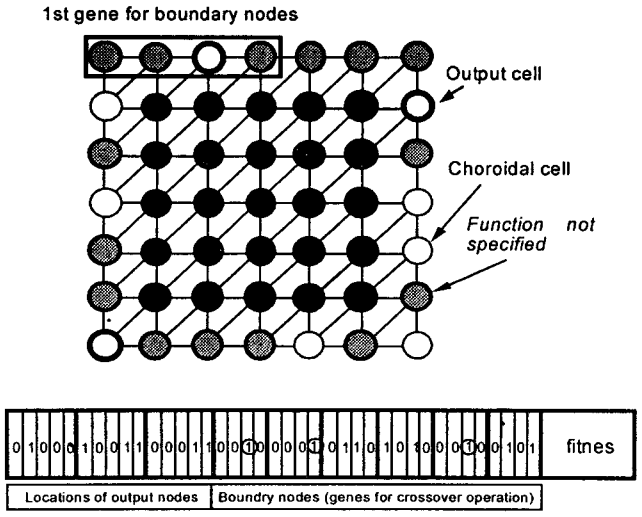

Fig. 6 An example of chromosome specifying the finite element retina.

Input Data Preparation for the Finite Element Retina Optimization

A growth of a community of radish sprouts was observed. The change of pictorial image due to the growth was recorded on a video tape. A digital still image was captured at a time from the video at intervals of 6 hours from seeding to 96 hours after seeding. Seventeen digital still images were obtained. Five out of 17 digital still images of the community of radish sprouts were processed to obtain input data for the finite element retina to be optimized as shown in fig. 7. The finite element features given by the three work cells of each finite element retina characterized by the corresponding chromosome in the GA optimization process were calculated using these five digital still images.

Fig. 8 illustrates the procedure to prepare input data for the finite element retina. The captured digital still image was divided into 5 × 5 segments. The image dimensions of each segment were 25 × 30 pixels. The average value of brightness (Y signal) of each segment was calculated. The calculate average brightness values made 25 input data which were fed into the finite element input nodes.

Evaluation of Optimized Finite Element Retina

Neural Network Model

A three-layered neural network was used to relate the growth of radish sprouts and the output of finite element features. The three-layered neural network with

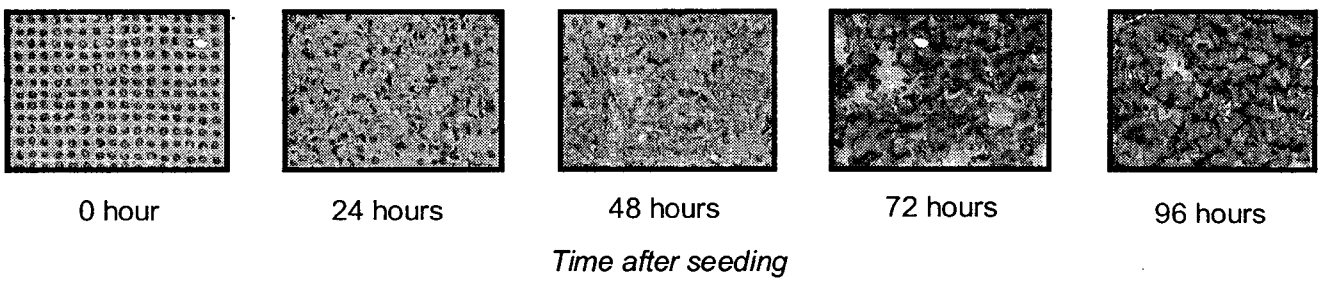

Fig. 7 Digital images showing changes in appearance of a community of radish sprouts.

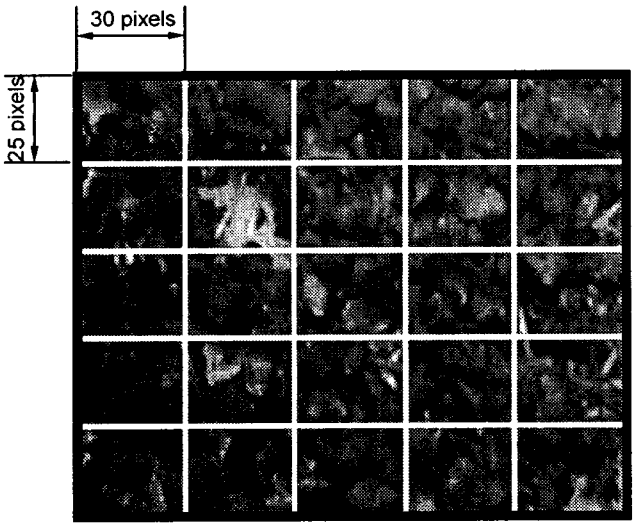

Fig. 8 Each captured image was divided into 25 segments. Average brightness of each segment was used for the input data for the finite element retina.

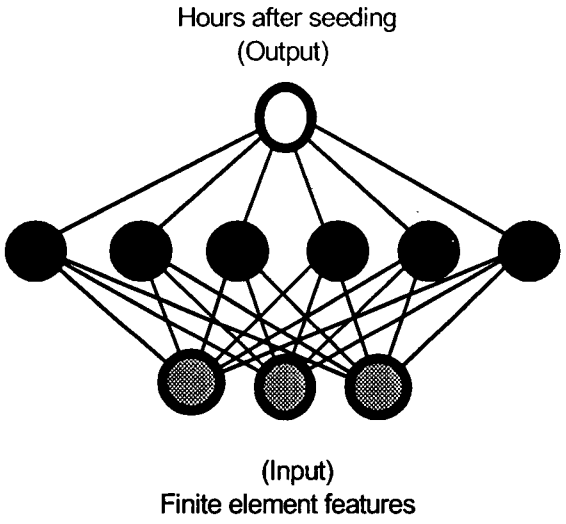

Fig. 9 Neural plant growth model.

the sigmoid non-linearity contains 6 units in the middle layer that makes the total number of units 10 as shown in fig. 9. The trained neural network is expected to estimate the growth stage of the community of radish sprouts based on the input data given by the finite element retina. A single output unit was provided for the hours after seeding. This neural network serves as a data convertor that transforms the three entities of the finite element features extracted from the pictorial image of plants into the growth stage of plants in terms of hours after seeding. The Kalman neuron training algorithm was applied for this problem.

Kalman Neuro Computing

The learning performance of neural network is of extreme importance for the users especially in a case where the training data contain significant amount of noise in measurement. The kalman filter can be used as a learning algorithm for the neural network. Fig. 10 illustrates an example of a three layered neural network structure. The mathematical explanation for the process of signal transfer in the network may help understand the mechanism of layered neural networks (Murase et al., 1991). The input T can be expressed in a vector form as $T=\{t_1,t_2,....,t_n\}$. I-th component of the inputs T, i.e., t_i that comes out from the input unit i is transferred to a hidden unit j through the synapse weight W_{ij}. Since each hidden unit has a summation function operating on inputs, the total input u_j received by the hidden unit becomes

$$u_j = \sum_{i=1}^{n} W_{ij}\, t_i \qquad (3)$$

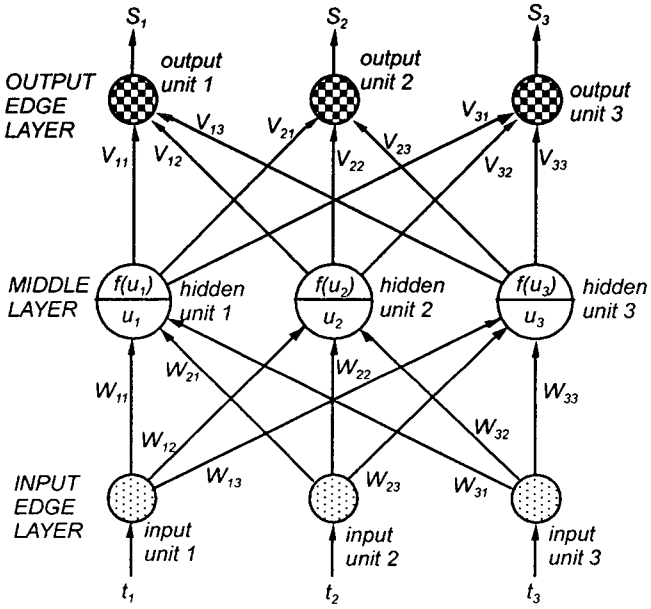

Fig. 10 Three-layered neural network structure.

The hidden unit i has also a transfer function that performs nonlinear transformation on the total input u_i and then gives an output which becomes the next input fed into the output unit j, which has also a summation function, throughout the synapse weight V_{ij}.

The total input received by the output unit j becomes directly its output s_j expressed as

$$s_j = \sum_{i=1}^{n} V_{ij}\, f(u_i) \qquad (4)$$

The outputs can be given in a vector form as $S=\{s_1,s_2,.....,s_m\}$. After all, what this neural network does is to perform a nonlinear transformation on T as expressed in the following equation.

$$S = F(T) \quad (5)$$

Once those nonlinear functions (transfer functions) of hidden units are specified, the behavior of the network can be identified by determining all synapse weights contained in the network. The sigmoid function is often employed for the transfer function. The learning of neural network is a procedure to determine optimal values of synapse weights by adjusting them step by step using known input data and their associated output data called training data. The most common algorithm for this learning procedure is the back propagation. The Kalman filter can also be used as a training algorithm. In this study, the Kalman filter algorithm was employed due to its quicker converging characteristics than any other algorithm (Murase, 1991). The state equation and the observation equation for the neural network can be described by the following forms:

1) State equation

$$\{x\}_{k-1} = [I]\{x\}_k \quad (6)$$

$\{x\}$: synapse weight to be determined

$[I]$: unit matrix

k : discrete time

2) Observation equation

$$\{y\}_k = \{h(\{x\})\}_k \quad (7)$$

$\{y\}$: unit values

$[h]$: observation matrix

The discrete time can be taken as the iterative step, i.e., learning iteration. The $[I]$ in eq. 6 is due to that synapse weight in this problem are independent of time. Eq. 7 is considered as a nonlinear observation equation that can be expressed in simpler form using the sensitivity matrix $[H]$ as given by eqs. 8, 9, and 10.

$$\{p\}_k = [H]_k\{x\}_k \quad (8)$$

where,

$$\{p\}_k = \{q\} - \{F(x,^t)_k + [H(x,^t)]_k\{X\}_k \quad (9)$$

$$[H_{ij}] = \partial F_i / \partial x_j \quad (10)$$

$\{q\}$: training data

X: synapse weights estimated at one step prior to the present iteration.

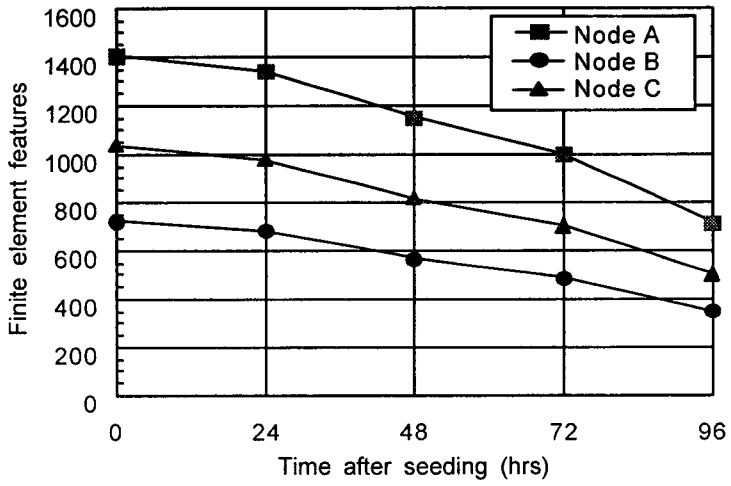

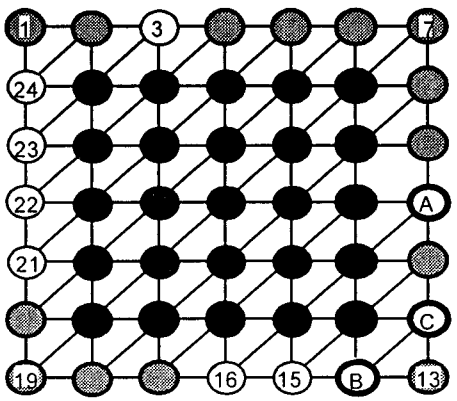

(a) Optimized finite element retina

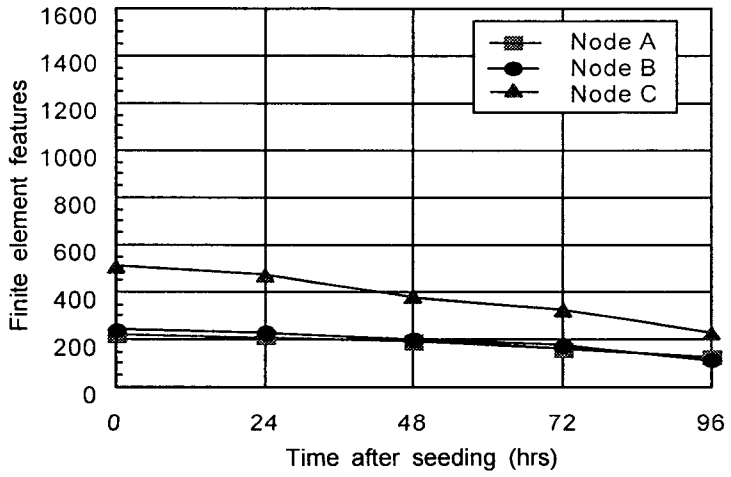

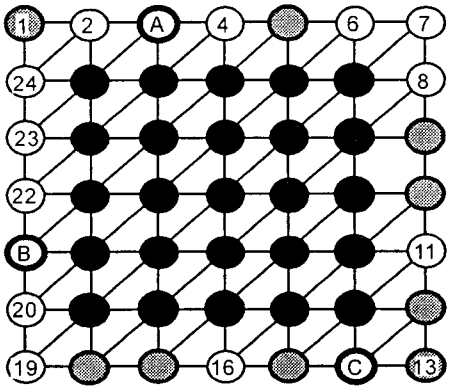

(b) Untreated finite element retina

Fig. 11 Comparison of finite element features obtained by the optimized retina (a) and untreated retina (b).

The observation vector $\{p\}$ and matrix $[H]$ can be evaluated using a priori information.

Training Data for the Finite Element Retina Evaluation

Two sets of training data were provided to make a comparison between an optimized finite element retina and an untreated finite element retina. One set of training data was obtained from an untreated retina and the other set of data from an optimized retina which is more sensitive to the change in the appearance of the growing plants through its digital image. During the 96-hour video taping, 17 image frames from 0 to 96 hours at 6-hour intervals were taken as described in the previous section. Three data obtained at 30 hours, 60 hours and 90 hours after seeding in each set of training data were left to be use for checking. The remaining 14 data of each data set were used for the neuron training.

Results and Discussion

After 52 iteration, the GA optimization converged to the best fitness. The structure of the optimized finite element retina and the variations of three image features (outputs) for the plant growth given by the optimized retina are shown in fig. 11(a). fig. 11(b) shows the structure of the finite element retina with the worst fitness chosen from chromosomes generated randomly at the initiation of the GA optimization and the plot of outputs versus the growth stage by time using the untreated retina. Less numbers of choroidal cell are allocated for the optimized retina. The plots in fig. 11 indicate that the optimized retina is much more sensitive to the changes in the appearance of growing plants through their digital images.

The learning process using the training data given by the optimized retina was terminated when the root mean squared error of outputs reached 3.12×10^{-3} after 500 times of iterative calculations. The root mean squared error of outputs converged to 9.84×10^{-2} for the untreated finite element retina also after 500 times of iterative calculations. The lower learning level attained by the training data given by the untreated finite element retina was probably due to the fact that the training data contained many output data of the untreated retina which remain almost unaffected by the variation of input data (digital image of plants). table 1 indicates satisfactory agreement of the estimated growth stage of radish sprouts with the actual measured data which was obtained by the neural plant growth model trained for the optimized finite element retina. The untreated finite element retina, in turn, gave unacceptable results as indicated in table 1.

Table 1 Comparison of estimated and actural values of plant growth stage indicated by time after seeding (hrs)

Actual	Estimates	
	Optimized	Untreated
30	28.1	16.3
60	60.7	55.9
90	91.0	92.9

Conclusions

Genetic algorithms can effectively optimize the performance of a finite element retina by improving the retinal sensitivity for tonal variation of digital image. It was found that an optimized finite element retina provides training data for building a better neural plant growth model than untreated finite element retina. The developed neural plant growth model is capable of estimating the plant growth stage based on time.

Acknowledgement

A research plant for extending this study has been accepted for a grant of the Ministry of Education, Science and Culture of Japan by a Grant-in-Aid for Developmental Scientific Research (Project No. 06556042).

References

Haralick, R. M., K. Shaanmugan and I. Dinstein. 1973. Textural features for image classification. IEEE Trans. on Systems, Man, and Cybernetics, Vol. SMC-3,6,610-621.

Hashimoto, Y. and N. Honami. 1992. Measurement and control in transplant production systems. In:Transplant Production Systems. (K. Kurata and T. Kozai, Ed.) pp 117-136. Kluwer Academic Publishers, Dordrecht, The Netherlands.

Murase, H., S. Koyama, N. Honami and T. Kuwabara. 1991. Kalman filter neuron training. Bull. Univ. Osaka Pref. Ser. B. 43,91-101.

Murase, H., N. Honami and Y. Nishiura. 1994. Image information feedback using textural features for plant growth control. Proc. of the First Asian Control Conference, Tokyo, July 27-30, 1994. Vol. 3, pp. 17-20.

Murase, H., Y. Nishiura and K. Mitani. 1995. Environ-

mental control strategies based on plant responses using intelligent machine vision technique. Proc. of the First IFAC/CIGR/EURAGENG/ISHS workshop on Control Applications in Post-Harvest and Processing Technology, Ostend, Belgium, June 1-2, 1995. pp 143-149.

Murase, H., Y. Nishiura and T. Suzuki. 1996. Extraction of non-parametric image features for plant growth control. Proc. of The 13th World Congress of IFAC, San Francisco, CA, USA. Vol. B. pp. 381-386.

Murase, H. and Y. Nishiura 1996. Finite element retina for plant growth monitoring. Acta Horticulturae, Accepted for publication.